Nanoscale

Accepted Manuscript

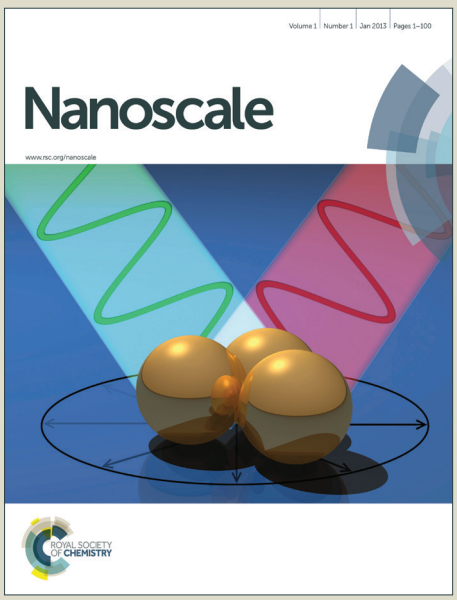

ROYAL SOCIETY OF CHEMISTRY

www.rsc.org/nanoscale

Cite this: DOI: 10.1039/c0xx00000x

www.rsc.org/xxxxxx

ARTICLE TYPE

Magnetic Resonance Imaging of Post-ischemic Blood-brain Barrier Damaging with PEGylated Iron Oxide Nanoparticles

Dong-Fang Liu, Chen Qian, Yan-Li An, Di Chang, Sheng-Hong Ju, Gao-Jun Teng*

Received (in XXX, XXX) Xth XXXXXXXXX 20XX, Accepted Xth XXXXXXXXX 20XX

DOI: 10.1039/b000000x

Blood-brain barrier (BBB) damaging during ischemia may induce devastating consequences like cerebral edema and hemorrhagic transformation. This study presents a novel strategy for dynamically imaging of BBB damaging with PEGylated supermagnetic iron oxide nanoparticles (SPIONs) as contrast agents. The employment of SPIONs as contrast agents made it possible to dynamically image the BBB permeability alterations and ischemic lesions simultaneously with T_2-weighted MRI, and the monitoring could last up to 24 h with a single administration of PEGylated SPIONs in vivo. The ability of the PEGylated SPIONs to highlight BBB damaging by MRI was demonstrated by the colocalization of PEGylated SPIONs with Gd-DTPA after intravenous injection of SPION-PEG/Gd-DTPA into a mouse. The immunohischemical staining also confirmed the leakage of SPION-PEG from cerebral vessels into parenchyma. This study provides a novel and convenient route for imaging BBB alteration in the experimental ischemic stroke model.

Introduction

Ischemic stroke continues to be one of the leading causes of disability or death worldwide[1]. Following cerebral ischemia, blood brain barrier damaging occurs due to basement membrane dissolution, active matrix metalloproteinases (MMP) release and inflammation[2], and consequently leads to an extravasation of high molecular weight molecules resulting in serious consequence like cerebral edema and hemorrhagic transformation[3-5]. Therefore, reliable imaging of BBB dysfunction is very important to both clinical and experimental research of ischemic stroke. Many efforts have been made to determine BBB functionality in ischemic brain tissues[6-10], in which MRI is considered to be a useful noninvasive tool to image BBB damaging visually and dynamically. Examination of BBB permeability by MRI is usually based on the monitoring of leakage of MR contrast agent, which can not cross an intact BBB, from brain vessels into parenchyma. Gadolinium-containing compounds, such as gadopentetate dimeglumine (Gd-DTPA), are frequently used as contrast agents[11], which enhance the contrast of MR images by shortening the longitudinal relaxation time (T_1) of MR signal. For example, Durukan et al. monitored BBB leakage by MRI for up to one week with Gd-DTPA as indicator [8]. Stoll et al. developed a MRI contrast agent gadofluorine M for in vivo detection of widespread BBB alterations[9]. Furthermore, MRI allows multiparametric studies of stroke by which other important parameters like anatomic images can be assessed. For example, T2-weighted imaging was usually used to demarcate cerebral ischemic lesions in many studies of BBB alterations to evaluate the correlation of BBB leakage with ischemic lesions[12].

Superparamagnetic iron oxide nanoparticles (SPIONs) have been demonstrated to be good MRI contrast agents, which can induce localized hypointense on T_2- or T_2*-weighted MR images due to the magnetic inhomogeneity generated by their strong magnetic moment[16]. SPIONs have significant advantages over other conventional paramagnetic agents (such as Gd-DTPA) at low concentrations due to their higher molar relaxivities[17]. Just like common nanomaterials, SPIONs are generally not able to cross BBB without the aid of ligands such as lactoferrin[18]. Accordingly, they are promising in the imaging of BBB damaging as MR contrast agents. However, SPIONs are prone to uptake by monocytes/macrophages. In view of this, to effectively image the BBB damaging with SPIONs, the nonspecific uptake of SPIONs by monocytes should be avoided prior to their reaching the ischemic cerebral tissue.

The pharmacokinetic properties of SPIONs can be tuned by surface modification. PEGylation has been frequently used to enhance the ability of nanoparticles to escape the reticuloendothelial system (RES) uptake. Various anchor groups including phosphate[19], carboxylate[20] and catechol[21,22] have been utilized for the PEGylation of SPIONs. It has been reported that high anti-biofouling ability can be achieved for the nanopartilces with dense PEG-coating, which can be introduced by the anchor groups with high binding affinity[21]. We have developed an effective method for the PEGylation of SPIONs, in which the poly(acrylic acid) (PAA) chains that are anchored to the surface of SPIONs through the robust collective coordination of multiple carboxylates provide plenty of carboxylic groups for the conjugation of high dense PEG chains to the SPIONs. The PEGylation achieved by this method affords the SPIONs good ability to resist the RES uptake[23]. In this study, we prepared PEGylated SPIONs with similar procedures, and studied their

application in dynamic imaging of BBB damaging after ischemic stroke with T_2-weighted MRI in a photochemically induced thrombosis (PIT) of proximal middle cerebral artery (MCA) mice model. After administration of the PEGylated SPIONs at 0.5 h after MCA occlusion, the monitoring of BBB changing can last for 24 h. With SPIONs as indicators, the information of BBB damaging and ischemic lesions can be imaged synchronously with one T_2-weighted MR sequence. For comparison, the images of BBB damaging and ischemic lesion have to be taken by T_1-weighted and T_2-weighted MR sequences respectively with Gd-based compounds as contrast agents. This study provides a convenient and time-saving route for BBB damaging analysis. To the best of our knowledge, this is the first case that SPIONs have been used as indicators of BBB damaging in the experimental ischemic stroke model. In the second instance, the evaluation of BBB alteration in ischemic stroke with T_2-weighted MRI is also lacking in the literature.

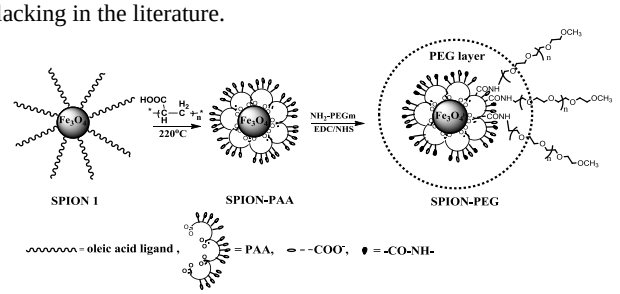

Scheme 1. Synthetic routes of SPION-PAA and SPION-PEG.

Results and discussion

Synthesis and Characterization of the PEGylated SPIONs

The PEGylated SPIONs were prepared following a reported method with slight modifications (see Experimental Section for detailed procedures) [23]. The structures and synthetic routes of SPION-PAA and SPION-PEG are schematically shown in Scheme 1. The PEGylation of SPION is characterized by the FT-IR spectrometry (Fig. 1). The absorption peak at ~1650 cm^{-1} in the FT-IR spectrum of SPIO-PEG (Fig. 1B), which is absent in the spectrum of SPION-PAA (Fig. 1A), can be assigned to the amide carbonyl groups introduced by the amidation of mPEG-NH_2 and PAA on the surface of SPION. The absorption band at 1109 cm^{-1} appears in the spectrum of SPION-PEG can be assigned to the stretching vibration of ether bond in PEG chains, that further confirmed the presents of the PEG coating on the SPIONs.

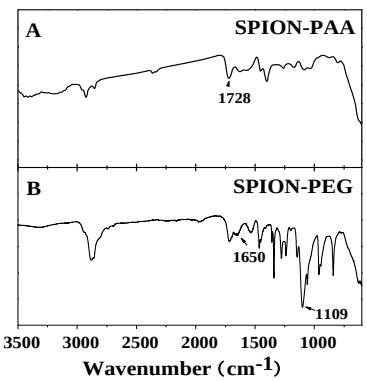

Fig. 1 FT-IR spectra of SPION-PAA (A) and SPION-PEG (B).

The morphology of the PEGylated SPION was studied by transmission electron microscopy (TEM). As shown in Fig. 2A, the diameter of the nanoparticles is in the range of 8-12 nm and no obvious aggregation is observed. The hydrodynamic diameter of the nanoparticles were measured to be 25 ± 3.6 nm with polydispersity index of 0.26 by dynamic light scattering (DLS) in aqueous medium.

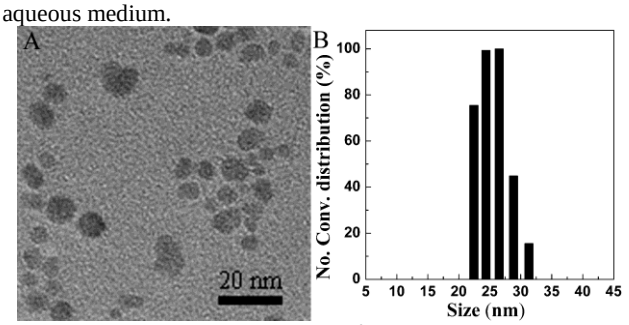

Fig. 2 (A) Representative TEM image of SPIO-PEG nanoparticles; (B) Hydrodynamic diameter distribution of SPION-PEG in distilled water.

The diagnostic abilities of the prepared SPION-PEG were assessed by determining the T_2 and T_1 of protons in SPION-PEG aqueous solutions. The results indicate that T_2-weighted MR signal intensity can be noticeably reduced by SPIO-PEG (Fig. 3A). The r_2 of SPION-PEG was calculated to be 92.7 mM^{-1} s^{-1} (Fig. 3C), which is high enough for MRI applications. SPION-PEG also induce decrease of MR signal intensity in the T_1-weighted image (Fig. 3B), and T_1 time of water protons was reduced in the presents of SPION-PEG. (r_1=0.84 mM^{-1} s^{-1}, fig. 3D).

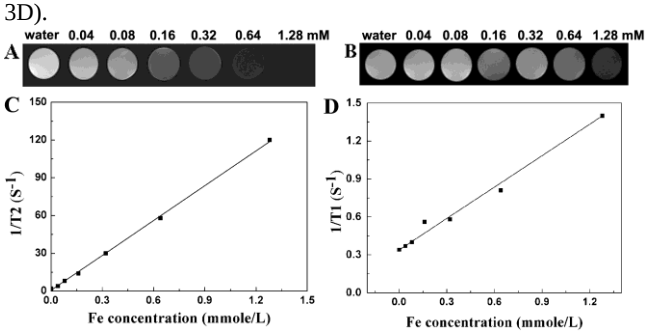

Fig. 3 (A) T_2-weighted and (B) T_1-weighted images of SPIO-PEG aqueous solutions at different concentrations; (C) T_2 relaxation rates ($1/T_2$) and (D) T_1 relaxation rates ($1/T_1$) plotted against the Fe concentrations of SPION-PEG.

In Vitro phagocytosis of the PEGylated SPIONs

RAW 264.7 mononuclear macrophages were used as model cells to evaluate the ability of SPION-PEG to resist the uptake by macrophages. Internalized nanoparticles were detected by Prussian blue staining and subsequent nuclear fast red counterstaining. It can be seen that the macrophages treated with SPION-PAA are stained in blue (Fig. 4A), indicating the uptake of the nanoparticles by the cells. As expected, no blue color can be observed in the macrophages treated with SPION-PEG (Fig. 4B), demonstrating that the phagocytosis of iron oxide nanoparticles by macrophages can be significantly suppressed by the PEGylation.

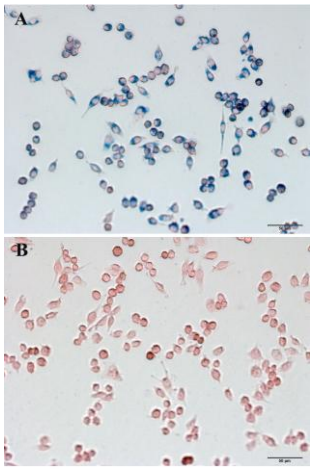

Fig. 4 Images of RAW 264.7 macrophages incubated with SPION-PAA (A) and SPION-PEG (B) after Prussian blue stain, the scale bar is 50 μm.

The toxicity of SPION-PEG was evaluated by the study of *in vitro* cytotoxicity of the nanoparticles against Raw 264.7 cells. The relative cell viabilities were measured after 24h of incubation with a series of doses of SPION-PEG from 5 to 100 μg Fe /mL by CCK-8 assay. The results (Fig. 5) demonstrated SPION-PEG has no significant cytotoxicity in the tested concentrations.

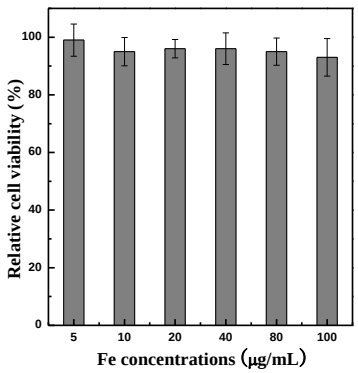

Fig. 5 *In vitro* cytotoxicity of SPION-PEG against RAW264.7 macrophages.

Blood concentration kinetics

To assess the blood distribution kinetics of the nanoparticles, SPION-PEG and SPION-PAA were injected *i.v.* into mice, respectively. Blood samples were collected at 5 min, 30 min, 1 h, 3 h, 6 h and 12 h post injection and the concentrations of Fe in serum were determined by Inductively Coupled Plasma-Atomic Emission Spectrometry (ICP-AES). For SPION-PEG, the amount of Fe in blood increases at initial stage and then decreases (Fig. 6), suggesting temporary iron storage in an organ during the first two hours after injection[24]. The half-life of SPION-PEG in blood circulation is calculated to be 204 min, while that of SPION-PAA is very short and calculated to be around 37 min.

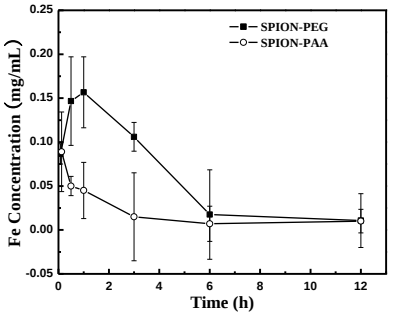

Fig. 6 Pharmacokinetics of SPION-PEG and SPION-PAA monitored by iron concentration in blood during 12 h. The iron concentration in the serum of the control blood samples is 0.004 ±0.002 mg/mL.

In Vivo MRI

In vivo MRI of SPION-PEG was conducted to assess its application potentials in imaging of BBB leakage by using C57 BL6-J mice with PIT of proximal MCA as model animals. A saline solution of SPION-PEG was injected into mice via tail vein at 0.5 h after PIT or sham-operated treatment at a dose normalized to be 10 mg Fe/kg body weight. For control experiments, SPION-PAA saline solution (the molar amount of Fe is equal to that of SPION-PEG) and saline alone were injected respectively into mice at 0.5 h after PIT treatment. T_2-weighted MR images acquired at pre- and scheduled temporal points post injection are presented in Fig. 7A. The ischemic lesions appear hyperintense in the T_2-weighted MR images and expand over the inspect time. The MR images exhibit a marked hypointense within the lesions at 1 h, 4 h, 8 h and 24 h post injection of SPION-PEG. In contrast, no obvious MR signal change is observed in the cerebral slices of the sham-operated mice injected with SPION-PEG, suggesting SPION-PEG can not pass through intact BBB, and thus the decrease of the T_2 signal intensity in the ischemic lesions can be ascribed to the leakage of SPION-PEG from broken BBB. The relative MRI signal changes (RSC, %) in the area of ischemic cerebral hemisphere indicated by the dashed circle are calculated to be about -27 ±4%, -45 ±9%, -33±10%, -21±6% at 1 h, 4 h, 8 h and 24 h post injection of SPION-PEG respectively with respect to pre-injection (Fig. 7B black column). Although the RSC decrease at 8 h and 24 h post injection, the area of hypointensity enlarged with the expansion of lesions (Fig. 7A), demonstrating the BBB damaging can be dynamically imaged up to 24 h with a single administration of SPION-PEG. In contrast, SPION-PAA give rise to little signal intensity decline comparing to saline in the ischemic cerebral hemisphere over the whole monitoring duration (Fig. 7B red and blue column), which should be ascribed to the nonspecific phagocytosis of SPION-PAA by monocytes/macrophages that have been reported to be recruited to ischemic lesions after 48 h of MCA occlusion[25], and the short blood circulation time of SPION-PAA (Fig. 6). The above results demonstrate that SPION-PEG reach the ischemic cerebral hemisphere via broken BBB, instead of monocytes uptake and recruition to ischemic lesions.

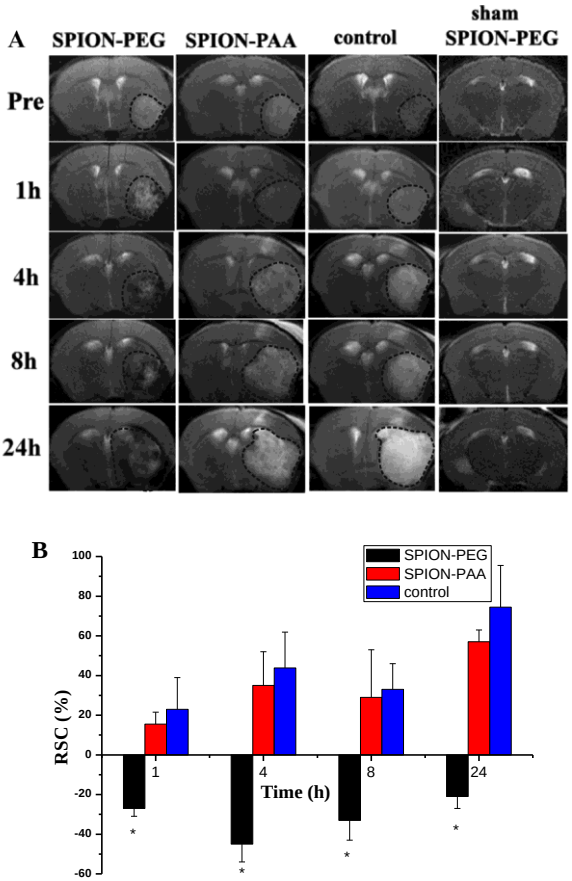

Fig. 7 (A) T_2-weighted images of brain of mice with PIT of proximal MCA and sham-operated at different time points post injection of 10 mg/kg of SPION-PEG, SPION-PAA and saline. (B) Relative signal intensity changes among different groups (n=3). * $P < 0.05$ *vs.* SPION-PAA and saline groups.

Gd-DTPA, which is a common clinical indicator of BBB damaging[11], was used for comparison with the effect of SPION-PEG on the imaging of BBB damaging. SPION-PEG solutions were injected into mice via tail vein at 0.5 h after PIT, and Gd-DTPA with 0.5 mmole/kg (287 mg/kg) body weights was injected 20 min before each time point of MR imaging to the same mouse for comparison. As shown in the T_1-weighted MRI in Fig. 8, both hyperintense and hypointense are observed in the same region indicated by the dashed circle at each time point of 2, 4, 6, 8 and 24 h post injection. The distribution of hypointensity is consistent with that in the corresponding T_2-weighted MRI, indicating the signal decrease in T_1-weighted MRI is induced by the accumulation of SPION-PEG. As the ischemic lesions show no signal change in T_1-weighted imaging[25], the hyperintense in the T_1-weighted images arise from passive diffusion of Gd-DTPA through broken BBB. The distribution of SPION-PEG and Gd-DTPA is not completely overlapped, which is probably due to the different diffusion ability of the nanoparticles and small molecules[26]. This result demonstrates the imaging of BBB damaging with SPION-PEG as indicator is comparable to that with Gd-DTPA as indicator at each time point in this ischemic stroke model, although the size of SPION-PEG is much larger than Gd-DTPA.

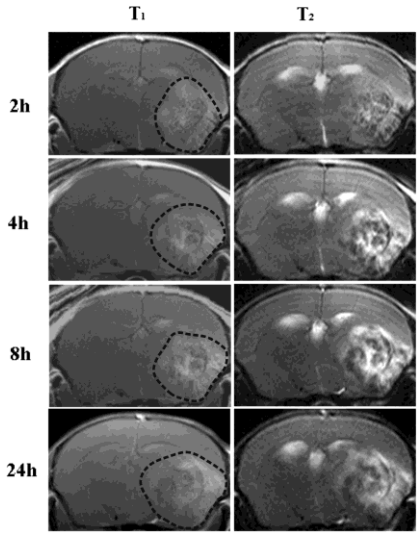

Fig. 8 T_1 and T_2-weighted MR images of mouse brain at different time points post injection of SPION-PEG with 287 mg/kg of Gd-DTPA injected at 20 min before each MR imaging.

Histology

Brain sections were sliced from the ischemic stroke mice at 24 h after the injection of SPION-PEG, SPION-PAA and saline respectively and stained by Prussian blue for ferric ions with nuclear fast red counterstaining. As shown in Fig. 9A, the accumulation of SPION-PEG in the ischemic cerebral hemisphere is confirmed by the presence of blue color stained by the Prussian blue staining. By contrast, little Fe can be detected by Prussian blue staining in the samples treated with SPION-PAA (Fig. 9B) and saline (Fig. 9C). This result consists well with the in vivo MRI analyses. To further verify the leakage of SPION-PEG from BBB, brain sections of the ischemic stroke mice treated with SPION-PEG were also stained successively by anti-CD31 antibody for cerebral vascular endothelial cells and Prussian blue for ferric ions. As shown in Fig. 9D, SPION-PEG is located in both vessels (indicated with black arrows) and paravasal parenchyma (indicated with red arrows) within the ischemic cerebral hemisphere. The present of SPION-PEG in the paravasal parenchyma indicates the leakage of SPION-PEG from the broken BBB.

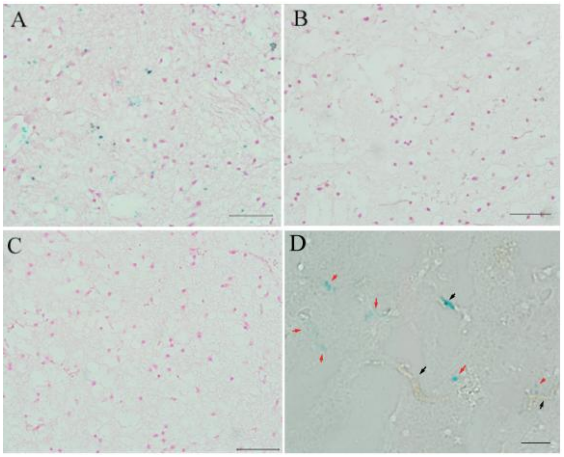

Fig. 9 Ex vivo Prussian blue and nuclear fast red double staining images of cerebral ischemic lesions excised from the mice at 24 h post-injection of SPION-PEG (A), SPION-PAA (B) and saline (C) respectively; (D) ex vivo anti-CD31 immunohistochemical and Prussian blue double staining images of cerebral ischemic lesions excised from the mice at 24 h post-injection of SPION-PEG; the scale bar of A, B, C is 50 μm, and D is 20 μm.

Conclusions

In conclusion, we have developed PEGylated SPION nanoparticles as an indicator for the BBB damaging in the PIT of MCA occlusion mice model. The BBB alteration after ischemic stroke can be dynamically monitored for 24 h with a single administration of SPION-PEG. The information of BBB permeability and ischemic lesions can be obtained simultaneously in a T_2-weighted MR image, and the detection efficiency of BBB damaging with SPION-PEG as contrast agents is similar to that with Gd-DTPA as contrast agents. This study provides a novel and complementary route for conveniently imaging of BBB damaging in the experimental ischemic stroke model.

Experimental Section

Materials

PAA (Mw≈1,800), EDC·HCl and NHS was purchased from Sigma-Aldrich Co. LLC and mPEG-NH_2 (Mw ≈ 2000) was purchased from Yarebio Co. Ltd, China. SPION 1 and SPION-PAA were prepared according to literatures[27,28]. SPION-PEG was prepared following the reported method with a little revision [23]. In brief, 100 mg of mPEG-NH_2 and 20 μL of triethylamine were added to a solution of 50 mg of SPION-PAA, 20 mg of EDC·HCl and 12 mg of NHS in 10 mL of water and the resulting mixture was stirred at room temperature for 2 h. Thereafter, 10 mL of DMF was added to the reaction mixture followed by removal of water under reduced pressure and subsequent addition of 40 mg of EDC·HCl and 24 mg of NHS. The resulting mixture was stirred for another 12 h. The crude product was purified by dialysis against water for 48 h.

Characterization

FT-IR spectra were measured on a Nicolet Nexus 870 FT-IR spectrometer. The morphologies of the nanoparticles were examined on a JEM-2000EX microscope. The hydrated diameter of SPION-PEG was measured on a 90 Plus Nanoparticle Size Analyzer, (Brookhaven Instruments Corp).in the 90° backscattering mode. The measurement was repeated for 3 times at 658.0 nm. The MR measurements were carried out on a 7 Tesla Micro-MRI (PharmaScan, Brukers, Germany) with a Bruker console (Bruker Biospin Inc.)

Measurement of MRI Relaxation Properties of SPION-PEG

The aqueous solutions of SPION-PEG with different concentrations were imaged at room temperature with a T_2 spin echo sequence (repetition time (TR) = 2000 ms, echo time (TE) = 13, 65 ms, field of view (FOV) = 40 mm×40 mm, slice thickness = 1 mm, matrix = 256 × 256) and T_1 spin echo sequence (TR = 500 ms, TE = 15 ms, FOV = 40 mm × 40 mm, slice thickness = 1 mm, matrix = 256 × 256) respectively. The T_1 and T_2 values were determined using a T_1 mapping sequence (TR = 2500 ms, TE = 11.01, 22.02, 33.03, 44.04, 55.05, 66.06, 77.07, 88.08, 99.09, 110.10, 121.11, 132.12, 143.13, 154.14, 165.15, 176.16 ms, FOV = 40 mm × 40 mm, slice thickness = 1 mm, matrix = 256 × 256) and a T_2 mapping sequence (TR = 5000, 3000, 1500, 800, 400, 200 ms, TE = 11 ms, FOV = 40 mm × 40 mm, slice thickness = 1 mm, matrix = 256 × 256). Relaxation rates were obtained from the slope of a linear fit of iron concentration (mM Fe) versus $1/T_1$ (s^{-1}) or $1/T_2$ (s^{-1}).

Blood half-life of SPION-PAA and SPION-PEG C57 BL6-J mice weighing about 20 g were employed in our study. Solutions of SPION-PEG or SPION-PAA were administered in mice respectively via tail vein at a dose normalized to be 10 mg Fe/kg body weight. 0.1–0.15 mL of blood samples were collected at each scheduled time points by retro-orbital puncture. Serum was obtained by centrifugation of the extracted blood samples. The iron concentrations in the serum samples were measured by ICP-AES after acid digestion.

Nanoparticles Uptake by Macrophages

RAW 264.7 macrophages (Shanghai Cell Bank, Chinese Academy of Sciences) were plated in a 24-well plate with a density of 10^5 cells/well. SPION-PAA and SPION-PEG were added into the cells respectively with a concentration of 0.3 mg Fe/mL. The cells were cultured for 2 h at 37 ℃ and then washed with PBS 3 times, and stained with Prussian blue staining for ferric ions with nuclear fast red counterstaining.

Cell toxicity assay

RAW264.7 macrophages were seeded in a 96-well plate with the density of 10^4 cells/well. The cells were cultured overnight and SPION-PEG with different concentrations was added into the cells. Each concentration was repeated for 3 times. After 24 h incubation, the cells were washed with PBS for three times and incubated with CCK-8 for another 1 h. The optical density of the solutions was measured with a microplate reader at 450 nm.

In Vivo MR Imaging

C57 BL6-J mice were anaesthetised with intraperitoneal injection of pentobarbital (6mL/kg, 1% in sterile saline). MCA was occluded with the PIT approach that has been reported elsewhere with a little modification[29]. After 0.5 h of PIT, nine mice were divided into three groups randomly and then administrated with saline solutions of SPION-PEG, SPION-PAA (10 mg/kg Fe equivalent), and saline respectively. Mice were anesthetized with a flow of isoflurane (1.5% vol. at 2 L/min) via a nose cone during the MR measurement. T_2-weighted spin echo MRI was acquired with TR/TE = 2000 ms/50 ms, FOV of 20 mm×20 mm, flip angle

162.9 °, slice thickness 1 mm and matrix 256×256. T1-weighted spin echo MRI was acquired with TR/TE = 500 ms /15 ms, FOV of 20 mm×20 mm, flip angle = 129.4 °, slice thickness 1 mm and matrix 256×256. The signal intensity (SI) was measured in the circled area of ischemic cerebral hemisphere. Relative signal change (RSC, %) was calculated according to the following formula: RSD % = 100× (SI post /SI pre), where SI pre and SI post indicate the signal intensity before and after each time point of SPION-PEG injection.

Comparison of SPION-PEG as indicators of BBB damaging with Gd-DTPA

Three C57 BL6-J mice with PIT of MCA occlusion received SPION-PEG (10 mg/kg) *i.v.* after 0.5 h of PIT. Thereafter, Gd-DTPA was injected (278 mg/kg body weight) at 20 min before each time point of MR imaging to the same mice. The mice were imaged at scheduled time points respectively with T_1- and T_2-weighted MR sequences respectively.

Statistical Analysis Comparison of RSC % among the groups treated with SPION-PEG, SPION-PAA and saline was determined by Student's t-test. P values less than 0.05 were considered statistically significant.

Histology Study

Mouse brain tissues were anatomized from the ischemic stroke mice at 24 h post injection of SPION-PEG, SPION-PAA and saline respectively. The tissues were fixed in 10% neutral buffered formalin and processed routinely into paraffin, sectioned at a thickness of 6 μm, double staining with Prussian blue and nuclear fast red.

For immunohistochemical study, the brain tissues from the stroke mice after 24 h injection of SPION-PEG were embedded in Tissue-Tek OCT compound, frozen and sectioned. The brain slices were stained successively with anti-CD31 antibody for cerebral vascular endothelial cells and Prussian blue for ferric ions.

Conflict of interest

The authors declare no competing financial interest.

Acknowledgements

This work was funded by National Program on Key Basic Research Project (Nos. 2013CB733804, 2013CB733803), General Program of Natural Science Foundation of Jiangsu Provence (BK20130057), Jiangsu provincial special program of medical science (BL2013029), National Natural Science Foundation of China (No. 81230034, 81101139, 81301270, 81271635).

Notes

Jiangsu Key Laboratory of Molecular and Functional Imaging, Department of Radiology, Medical School, Zhongda Hospital, Southeast University , No. 87, Dingjiaqiao, Nanjing, China 210009, Fax: +86-25-83272541; Tel: +86-25-83272121; E-mail: gjteng@vip.sina.com.

Reference

1. J. A. Chalela, J.G. Merino and S. Warach, *Curr Opin Neurol*. 2004, **17**: 447.
2. R. Brouns and P.P. DeDeyn, *Clin Neurol Neurosurg*. 2009, **111**: 483.
3. M. Spatz. *Acta Neurochir Suppl*. 2010, **106**: 21.
4. K. E. Sandoval and K. A. *Neurobiol Dis.* 2008, **32**: 200.
5. S. Taheri, E. Candelario-Jalil, E. Y. Estrada and G. A. Rosenberg, *PLoS ONE*. 2009, **4**: e6597.
6. W. Liu, J. Hendren, X. J. Qin, J.Shen, K and J. Liu, *J. Neurochem.* 2009, **108**: 811.
7. D. Michalskia, J. Groscheb, J. Pelza, D. Schneider, C. Weise, U. Bauer , J. Kacza, U. Gärtner, C. Hobohm and W. Härtig, *Brain Res.* 2010, **1359**: 186.Fi
8. G. Stoll, C. Kleinschnitz, S. G. Meuth, S. Braeuninger, C. W. IP, C. Wessig, I. Nölte and M. Bendszus, *J Cerebr Blood F Met*. 2009, **29**: 331.
9. A. Durukan, I. Marinkovic, D. Strbian, M. Pitkonen, E. Pedrono, L. Soinne, U. Abo-Ramadan, T. Tatlisumak, *Brain Res*. 2009, **1280**: 158.
10. Y.Z. Qu, , M. Li, Y.L. Zhao, Z.W. Zhao, X.Y. Wie, J. P. Liu, L. Gao and G. D. Gao, *Eur. J. Pharmacol.*2009, **606**: 137.
11. K. Schokland and H. shalev, *Epilepsia* 2012, **52 (Suppl. 6)**: 7.
12. T. N. Nagaraja, R. A. Knight, J. R. Ewing, K. Earki, V. Nagesh, and J. D. Fenstermacher, In: Nag S, *The blood-brain and other neural barriers, 9 ed*. Berlin: Springer, 2011, 193.
13. D. Artemov, *J Cell Biochem.* 2003, **90**: 518.
14. K. Park, S. Lee, E. Kang, K. Kim, K. Choi and I. C. Kwon, *Adv. Funct. Mater*. 2009, **19**: 1553.
15. R. Qiao, C. Yang and M. Gao, *J. Mater. Chem.* 2009, **19**: 6274.
16. J. W. Bulte, J. Vymazal, R. A. Brooks, C. Pierpaoli and J. A. Frank, *J. Magn. Reson. Imaging*. 1993, **3**: 641.
17. I. Akira, S. Masashige, H. Hiroyuki and K. J. Takeshi, *J. Biosci. Bioeng.* 2005, **100**: 1.
18. R. Qiao, Q. Jia, S. Hüwel, R. Xia, T. Liu, F. Gao, H.- J. Galla and M. Gao, *ACS nano*. 2012, **6**: 3304.
19. U. I. Tromsdorf, O. T. Bruns, S. C. Salmen, U. Beisiegel and H. Weller, *Nano Lett*. 2009, **9**: 4434.
20. Q. L. Fan, K. G. Neoh , E. T. Kang , B. Shuter and S. C. Wang, *Biomaterials* 2007, **28**: 5426.
21. E. Amstad, T. Gillich, I. Bilecka, M. Textor and E. Reimhult, *Nano Lett.* 2009, **9**: 4042.
22. E. Amstad, S. Zurcher, A. Mashaghi, J. Y. Wong, M. Textor and E. Reimhult, *Small* 2009, **5**: 1334.
23. D. Liu, , W. Wu, , J. Ling, , S. Wen, N. Gu, and X. Zhang, *Adv Funct Mater*. 2011, **21**: 1498.
24. A. Ruiz, Y. Hernández, C. Cabal, E. González, S. Veintemillas-E.Verdaguer and M. P.Martínez, *Nanoscale* 2013, **5**: 11400.
25. M. Rausch, D. Baumann, U. Neubacher and M. Rudin, *NMR biomed*. 2002, **15**: 278.
26. R. K. Jain and T. Stylianopoulos, *Nat Rev clin Oncol*. 2010, **7**: 653.
27. W. M, Zheng, F. Gao, H. C. Gu. *J Magn Magn Mater.* 2005, **288**: 403.
28. T. Zhang, J. Ge, Y. Hu and Y. Yin, Nano Lett. 2007, **7**: 3203.
29. F. Chen, Y. Suzuki, N. Nagai, X. Suna, W. Coudyzer, J. Yu, G. Marchal and Y. Ni, *Euro J Radiol*. 2007, **61**: 70.

